



Article

DGNCA-Net: A Lightweight and Efficient Insulator Defect Detection Model

Qiang Chen ¹, Yuanfeng Luo ¹, Wu Yuan ¹, Ruiliang Zhang ² and Yunshou Mao ^{3,*}

- ¹ Baise Bureau CSG EHV Power Transmission Company, Baise 533000, China
- ² Guiyang Bureau CSG EHV Power Transmission Company, Guiyang 550081, China
- School of Electronic Information and Electrical Engineering, Huizhou University, Huizhou 516007, China
- * Correspondence: maoyunshou@163.com

Abstract

This paper proposes a lightweight DGNCA-Net insulator defect detection algorithm based on improvements to the YOLOv11 framework, addressing the issues of high computational complexity and low detection accuracy for small targets in machine vision-based insulator defect detection methods. Firstly, to enhance the model's ability to perceive multi-scale targets while reducing computational overhead, a lightweight Ghost-backbone network is designed. This network integrates the improved Ghost modules with the original YOLOv11 backbone layers to improve feature extraction efficiency. Meanwhile, the original C2PSA module is replaced with a CSPCA module incorporating Coordinate Attention, thereby strengthening the model's spatial awareness and target localization capabilities. Secondly, to improve the detection accuracy of small insulator defects in complex scenes and reduce redundant feature information, a DC-PUFPN neck network is constructed. This network combines deformable convolutions with a progressive upsampling feature pyramid structure to optimize the Neck part of YOLOv11, enabling efficient feature fusion and information transfer, while retaining the original C3K2 module. Additionally, a composite loss function combining Wise-IoUv3 and Focal Loss is adopted to further accelerate model convergence and improve detection accuracy. Finally, the effectiveness and advancement of the proposed DGNCA-Net algorithm in insulator defect detection tasks are comprehensively validated through ablation studies, comparative experiments, and visualization results.

Keywords: insulator defect detection; lightweight model; improved Ghost module; Coordinate Attention; progressive upsampling feature pyramid



Academic Editor: Frank Werner

Received: 21 June 2025 Revised: 2 August 2025 Accepted: 14 August 2025 Published: 20 August 2025

Citation: Chen, Q.; Luo, Y.; Yuan, W.; Zhang, R.; Mao, Y. DGNCA-Net: A Lightweight and Efficient Insulator Defect Detection Model. *Algorithms* 2025, 18, 528. https://doi.org/ 10.3390/a18080528

Copyright: © 2025 by the authors. Licensee MDPI, Basel, Switzerland. This article is an open access article distributed under the terms and conditions of the Creative Commons Attribution (CC BY) license (https://creativecommons.org/licenses/by/4.0/).

1. Introduction

As a critical component of power transmission lines, insulators play a key role in ensuring safe isolation from grounded structures and maintaining the stable operation of the power grid. However, due to harsh environmental conditions and natural weather disasters such as strong winds, heavy rain, snow, and high temperatures, insulators are prone to defects like self-explosion, string drop, damage, and flashover discharge. These defects not only compromise the integrity of the insulators but can also lead to power safety incidents [1–3]. Moreover, the complex environments where transmission lines are located often feature diverse and cluttered backgrounds, including trees, buildings, and utility poles, which further increase the difficulty of defect detection. Therefore, timely

and accurate detection of defects in transmission line insulators is an essential measure for ensuring the safety of the power system.

In the early stages, insulator defect detection relied on manual inspection, which was not only labor-intensive and time-consuming but also lacked reliability in detection quality. In recent years, with technological advancements, machine vision-based methods have become the primary approach for insulator defect detection due to their high real-time performance and accuracy [4–10]. For example, utilizing drone-captured images enables the timely and precise identification of damaged insulators. Currently, the two mainstream methods for machine vision-based insulator defect detection are the lightweight deep learning model design [11–19] and feature extraction frameworks optimization [20–25].

Dahua Li et al. [11] proposed a LiteYOLO-ID insulator defect detection model with strong generalization ability by designing a new lightweight convolution module ECA-GhostNet-C2f and a neck network EGC PANet. Yanping Chen et al. [12] made lightweight improvements to the backbone network Faster R-CNN, greatly reducing model parameters and improving its detection accuracy. Zhibin Qiu et al. [13] used a MobileNet lightweight convolutional neural network to optimize the YOLOv4 model structure, enhancing the accuracy and speed of insulator defect detection. Zhong Cao et al. [14] introduced CAM and CSO into the original YOLOv8m, improving detection accuracy and reducing model parameters. Yang Lu et al. [15] designed a lightweight attention mechanism and introduced GSConv and C3Ghost convolution modules to reduce redundant parameters in the model. Yong Jiang et al. [16] adopted a new lightweight module C2f-RBE in the backbone architecture, which replaces traditional bottlenecks with RepViTBlocks and significantly improves detection efficiency and performance. Cong Liu et al. [17] integrated the Ghost module and introduced C3Ghost as an alternative to the backbone network, proposing a lightweight detection algorithm for multiple defects in insulators based on an improved YOLOv5s. Weiyu Han et al. [18] improved the C2f module by introducing the SCConv module, thereby enhancing the backbone network, reducing space and channel redundancy, and lowering computational complexity and parameter count. Liangliang Wei et al. [19] proposed an automatic detection method based on an improved lightweight YOLOv5s model and used GIoU loss function, Mish activation function, and CBAM module to identify and locate insulator defects.

Zheng He et al. [20] integrated the Adaptive Feature Fusion (ASFF) module, which enables the network to learn the relationships between different feature maps, enhance semantic information, and improve the network's ability to detect minor defects. Qiang Zhang et al. [21] constructed the C3 Global Pool Fusion (C3-GPF) module, aiming to enhance the focus on key data in the extraction and fusion stages of insulator defect features. Chuang Gong et al. [22] enhanced the C2f structure of YOLOv8 and improved its multi-scale feature extraction and multi-level feature fusion capabilities by integrating the expansion direction residual module and heavy parameter module. Bao Liu et al. [23] introduced spatially aware convolution in the task and structure dual decoupling head regression branch, enhancing the ability to extract spatial feature information in both horizontal and vertical directions. Zhongsheng Li et al. [24] replaced the traditional PANet structure with a BiFPN-P feature fusion module to improve the extraction of shallow features. Zhuye Xu et al. [25] proposed a new attention mechanism (MAP-CA) that effectively integrates global and local feature information by combining mean pooling and max pooling, achieving higher accuracy in insulator defect recognition.

Although the above studies have achieved valuable results, there are contradictions between model complexity and recognition accuracy in [11–19], and the manually optimized feature extraction methods in [20–25] have limited generalization ability.

Algorithms 2025, 18, 528 3 of 17

Moreover, current mainstream object detection algorithms still face significant challenges in small object recognition. For instance, YOLOv5s only achieves a mAP of 21.5% for small objects (area $< 32 \times 32$) on the COCO dataset, which is substantially lower than its performance on medium (44.6%) and large objects (56.2%) [26]. YOLO models often exhibit low accuracy and sensitivity to background noise in small object detection, where deeper networks may cause small object features to be lost or suppressed [27]. Since insulator defects often appear in small sizes and concealed forms, existing methods struggle to balance detection accuracy and efficiency, particularly in scenarios with complex backgrounds and low contrast. In light of this, this paper proposes an improved DGNCA-Net insulator detection framework based on YOLOv11 [28], featuring a lightweight Ghost backbone as its core backbone network. The primary contributions of this paper can be summarized as follows.

- (1) Deformable convolution (DC) with GhostNet combined in parallel with a 3 × 3 convolution to form the Large-Kernel Deformable Ghost Parallel Convolution (LKDGPC) module, which replaces original convolution layers in YOLOv11.
- (2) A DGhost-C3K (DG-C3K) module is developed based on the Deformable Ghost (DGhost) module to replace the original C3K2 module, aiming to improve feature extraction efficiency and representation.
- (3) A Cross Stage Partial Coordinate Attention (CSPCA) module is introduced to replace the C2PAS module in the backbone's final stage, enhancing object localization capabilities.
- (4) A Progressive Upsampling Feature Pyramid Network (PUFPN) with deformable convolution is proposed as a redesigned neck (DC-PUFPN), enabling better feature fusion and improved detection of small insulator defects.

The structure of this article is organized as follows: Section 2 provides a comprehensive introduction and analysis of the proposed model. Section 3 presents detailed quantitative and qualitative experimental results, validates the effectiveness of each component through ablation studies, and demonstrates the superiority and advanced performance of the proposed model through comparative experiments. Finally, Section 4 concludes the article and summarizes the main findings and key insights.

2. DGNCA-Net Insulator Defect Detection Model

YOLOv11 is a model based on the Cross Stage Partial Network (CSPNet) architecture, with its core being the C3K2 module, which is an improved version of the C2F module in YOLOv8. The backbone network and neck network adopt CNN and Path Aggregation Network (PANet) structures, respectively. However, both the CNN model and the PANet structure have shortcomings such as insufficient global feature extraction ability and repeated feature fusion, resulting in low detection accuracy and excessive computational redundancy. In light of this, this paper improves the feature extraction, feature fusion, and loss function components based on the YOLOv11 framework, proposing an efficient and lightweight DGNCA-NET insulator defect detection algorithm. The model framework is shown in Figure 1:

Algorithms **2025**, 18, 528 4 of 17

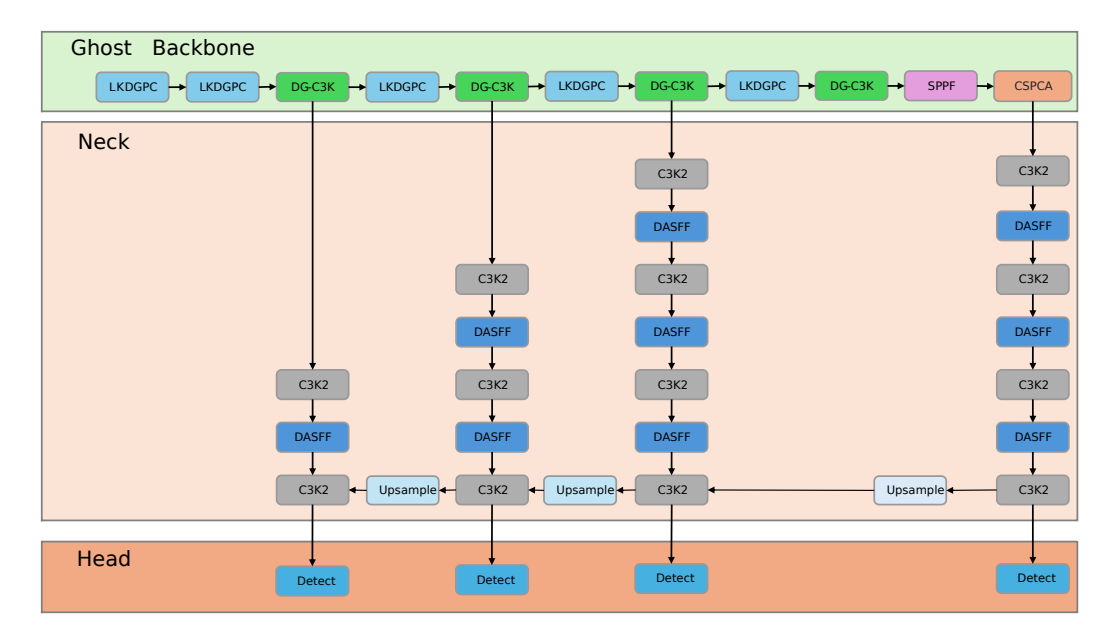


Figure 1. DGNCA-NET model framework.

2.1. Large-Kernel Deformable Ghost Parallel Convolution Block

Traditional CNNs suffer from high computational redundancy and insufficient model lightweighting during feature extraction, making it difficult to meet the efficiency requirements of real-time detection tasks. Despite continuous advancements in exploring lightweight network structures, the key challenge remains how to reduce the number of parameters while maintaining or even enhancing feature representation capabilities.

Inspired by [29,30], this paper proposes an LKDGPC module (as shown in Figure 2) that employs 31 × 31 large-kernel convolution and DGhost for dual-path feature extraction. LKDGPC feeds input features into two branches: One is a large-kernel convolution with a large receptive field, which significantly enhances the network's ability to capture multi-scale contextual information. It addresses the limited receptive field of small-kernel convolution layers, thereby improving the detection of insulator defects at various scales, while also partially mitigating the optimization difficulties associated with increased model depth. The other branch is a lightweight DGhost module that efficiently generates diverse and rich local detail features through cheap linear operations, enhancing sensitivity to subtle and small-scale defects while keeping computational cost low. Finally, the features from the two branches are concatenated and fused, balancing broad spatial context with fine-grained details. Moreover, the deformable convolution in the large-kernel branch dynamically adjusts sampling positions, boosting the model's adaptability to geometric transformations and irregular shapes common in insulator defects. Compared to the replaced standard convolutions, this architectural change not only improves multi-scale perception and local feature extraction but also reduces overall parameter count and computational complexity, leading to better detection accuracy and faster inference.

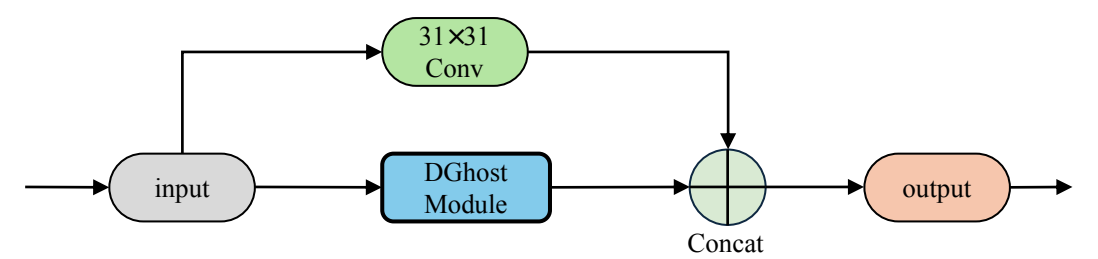


Figure 2. Large-Kernel Deformable Ghost Parallel Convolution Block.

Algorithms **2025**, 18, 528 5 of 17

The DGhost module is an improved variant of the core component in GhostNet, namely the Ghost module. The fundamental design philosophy of this module is to generate informative and discriminative Ghost feature maps from the original feature maps through a series of cheap linear operations, which significantly reduces computational cost and parameter count while maintaining competitive performance.

As illustrated in Figure 3, the DGhost module integrates both standard convolution and lightweight linear operations. Specifically, a portion of the input feature maps is first processed through standard convolution to produce intrinsic features. The remaining features are then generated by applying multiple cheap linear transformations to the intrinsic ones. Finally, these two sets of features are concatenated to form the complete output feature map. Compared to conventional convolutional operations, the DGhost module enables more diverse and informative feature representations at a significantly lower computational cost, thereby improving the inference efficiency and deployment friendliness of the network.

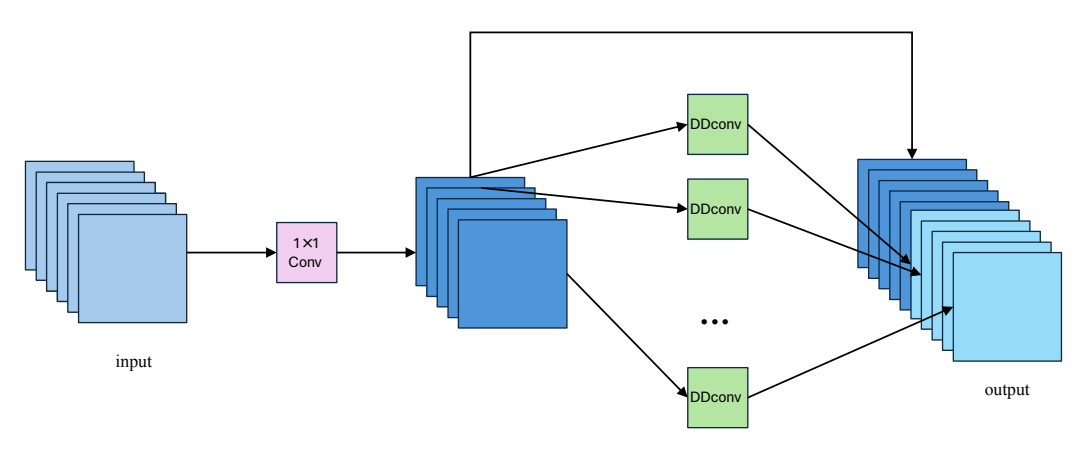


Figure 3. Deformable Ghost module.

On top of this, the DGhost module further modifies the original Ghost module by introducing DC (as shown in Figure 4) into the original depthwise convolution, forming a deformable depthwise convolution (DDConv). This enhancement allows the module to better model geometric transformations and complex object structures. By dynamically adapting the sampling locations, DC increases the spatial flexibility of the convolution operation, thereby enabling the network to more effectively capture irregular object shapes and deformations.

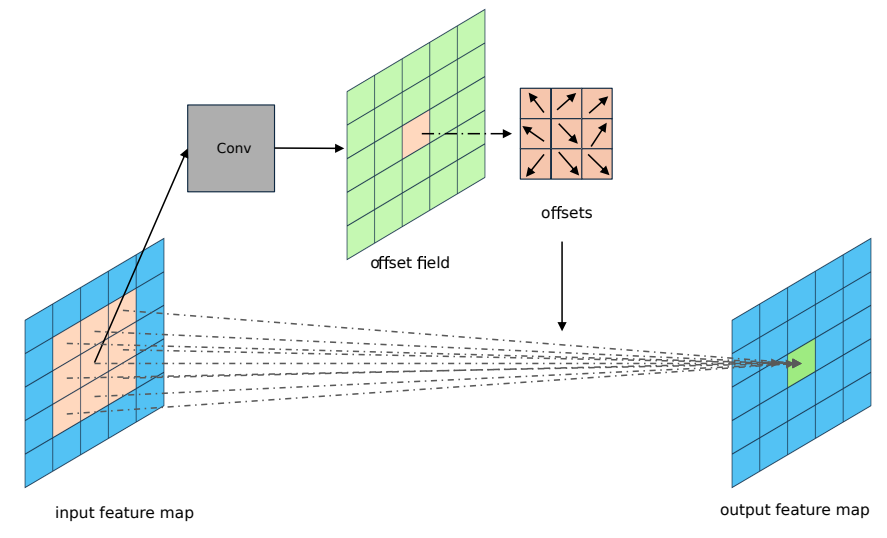


Figure 4. Deformable convolutional structure.

Algorithms **2025**, 18, 528 6 of 17

For any point p_0 on the input feature map, the traditional convolution operation can be expressed as follows:

$$y(p_0) = \sum_{p_n \in R} \omega(p_n) x(p_0 + p_n)$$
 (1)

where $\omega(p_n)$ is the convolution kernel weight at this position, $x(\cdot)$ is the input feature map, and p_n represents the offset of each point in the convolution kernel relative to the center point.

In DC, an additional offset Δp_n is introduced for each point, the convolution operation of DC can be expressed as follows:

$$y(p_0) = \sum_{p_n \in R} \omega(p_n) x(p_0 + p_n + \Delta p_n)$$
 (2)

2.2. DGhost-C3K3 Block

The C3K2 module is a key component in the YOLOv11(as shown in Figure 5a). It is an enhanced version based on the traditional C3 module, designed to improve feature extraction capabilities. However, the convolutional kernel size in C3K2 is fixed, making it difficult to capture large-scale or elongated insulator features and to model long-range dependencies. Additionally, the standard convolution's spatial sampling is too regular, failing to dynamically align with irregular cracks, pits, and other deformations on the insulator surface, which results in challenges in precisely locating tiny defects.

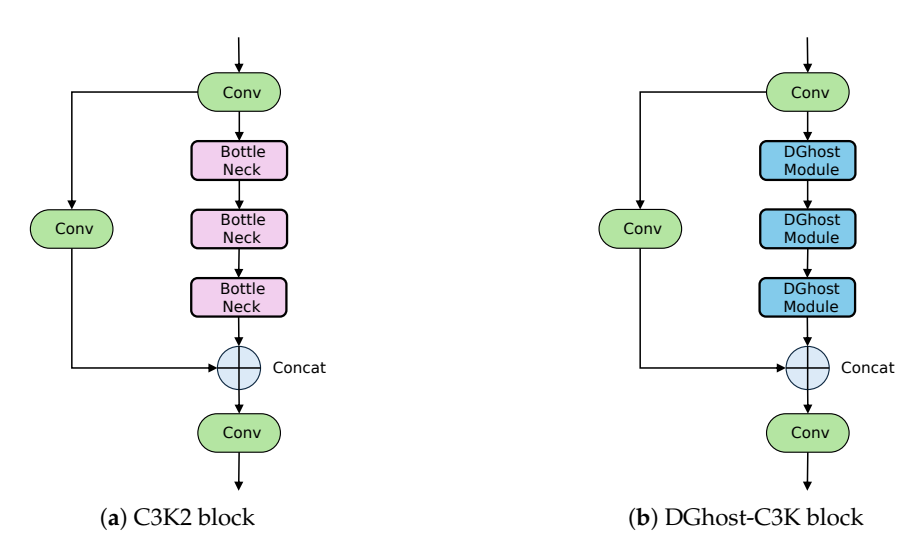


Figure 5. Comparison between C3K3 and DGhost-C3K.

In light of this, this paper proposes a DG-C3K3 module (as shown in Figure 5b), which replaces the bottleneck in the original C3K2 with a DGhost module. This architectural change brings several concrete advantages. First, by integrating deformable convolution within the DGhost module, the DG-C3K3 can dynamically adjust sampling positions based on the insulator surface texture, enabling more flexible spatial sampling that better aligns with irregular cracks, concave—convex edges, and other complex geometric deformations. This flexibility overcomes the fixed, rigid sampling grid of the original C3K2, improving the network's ability to precisely capture fine-grained defect features. Second, the Ghost mechanism inside the DGhost module efficiently generates diverse and informative feature maps through inexpensive linear transformations, which enhances feature richness and discrimination without a large computational burden. Although the inclusion of deformable convolution slightly increases the parameter count, the Ghost mechanism compensates by significantly reducing redundant computations in feature generation. Overall, this replace-

ment enhances the module's adaptability to irregular defect shapes, improves multi-scale and long-range feature representation, and achieves substantial performance gains with only minimal computational overhead.

2.3. Cross Stage Partial Coordinate Attention Block

In the YOLOv11 model, as the network depth increases, deep feature extraction faces challenges such as information loss and insufficient semantic representation. The attention mechanism in the original C2PSA module (as shown in Figure 6a) has limited capability in fusing spatial positional information and channel features, making it difficult to effectively capture fine-grained structures and long-range dependencies of the target. This results in imprecise deep feature representations, thereby affecting the model's detection performance in complex scenarios.

To address this issue, this paper replaces the Pyramid Split Attention mechanism in the C2PSA module with Coordinate Attention and proposes a new set of CSPCA modules (as shown in Figure 6b) to enhance the model's ability to capture and represent deep semantic features more effectively.

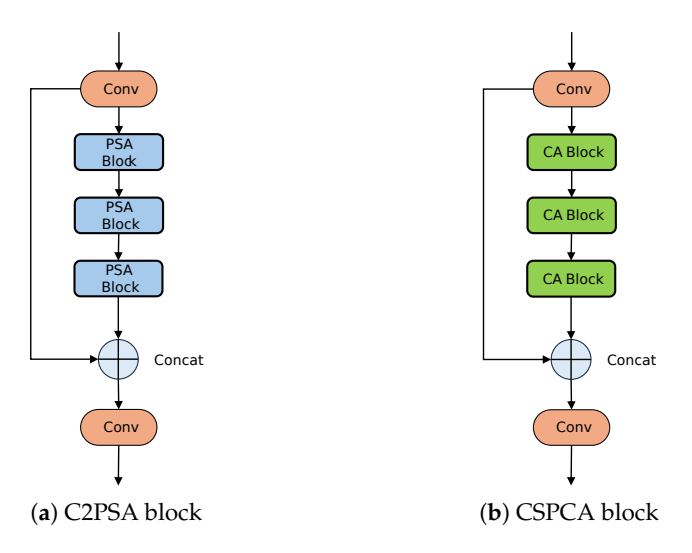


Figure 6. Comparison between C2PSA and CSPCA.

The CA block (as shown in Figure 7a) consists of convolution and a Coordinate Attention (CA) module, achieving feature enhancement through feature concatenation and residual connections. The coordinate attention mechanism first applies channel-wise attention weighting to the input features, followed by spatial coordinate-aware optimization to refine feature representation. Finally, it fuses the refined features with the original ones to improve the model's ability to capture both the target's location and semantic information.

The Coordinate Attention block (as shown in Figure 7b) is based on a residual structure. It first performs average pooling along the horizontal and vertical directions to capture long-range spatial dependencies. The pooled features are then concatenated and passed through a series of operations including convolution, normalization, and non-linear activation to generate attention weights for both horizontal and vertical directions. These weights are finally fused with the residual branch to produce the output. By decoupling attention along the horizontal and vertical dimensions, the module can precisely locate the target's row and column positions, effectively enhancing feature extraction for insulators of various scales and poses, while also reducing computational redundancy.

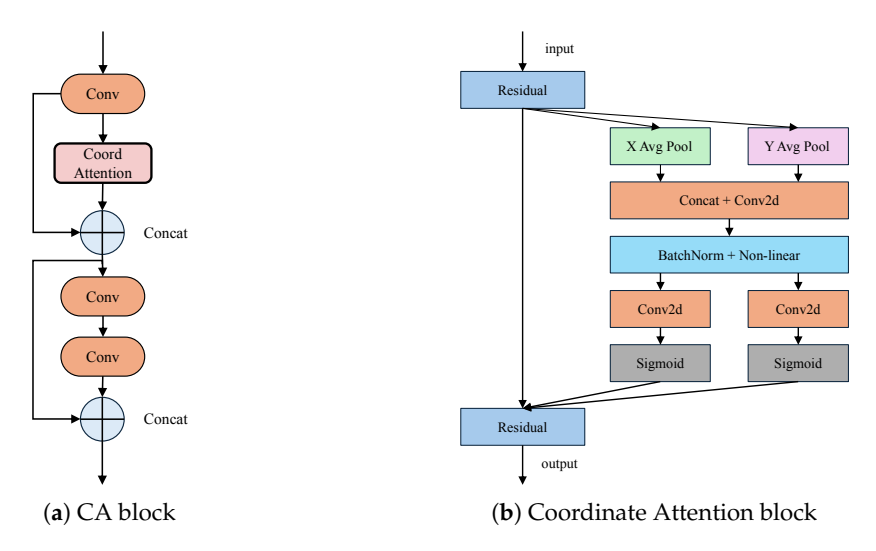


Figure 7. CA block and Coordinate Attention block.

2.4. DC-PUFPN Block

The neck network of YOLOv11 adopts the PANet structure, which has the drawback of using a static weight fusion strategy for feature fusion, lacking dynamic adaptability. This makes it difficult to adjust the feature fusion strategy according to the input content, leading to being unsuitable for small-object detection tasks. Meanwhile, PANet repeatedly performs feature fusion, generating a large amount of redundant information and increasing computational overhead. This paper proposes a PUFPN structure (see Figure 8), which adopts a unidirectional, progressive upsampling fusion strategy to reduce redundant processing. By orderly controlling the number of upsampling operations, the structure effectively reduces computational redundancy and memory consumption. The fused features at each scale are directly fed into the corresponding detection head, avoiding feature contamination caused by repeated transmission. This structure enables accurate recognition of targets at different scales in insulator images.

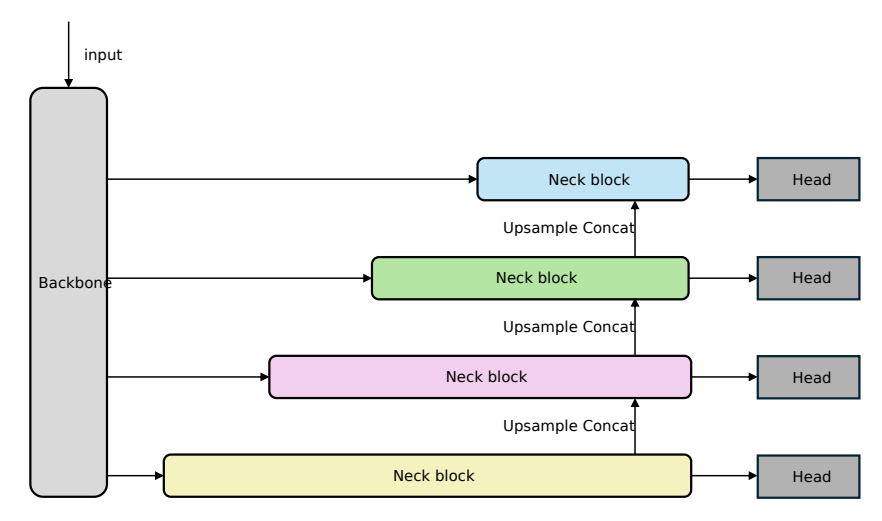


Figure 8. Progressive upsampling feature pyramid network.

In addition, the PUFPN structure employs the Adaptive Spatial Feature Fusion (ASFF) module (see Figure 9a) for feature fusion. Building on this, this paper introduces further improvements by drawing inspiration from the optimization strategies used in the Backbone network. Specifically, the standard convolution layers in the ASFF module are replaced with DC, resulting in the proposed Deformable Adaptive Spatial Feature Fusion (DASFF) module (see Figure 9b), which enhances the network's ability to model spatial structures.

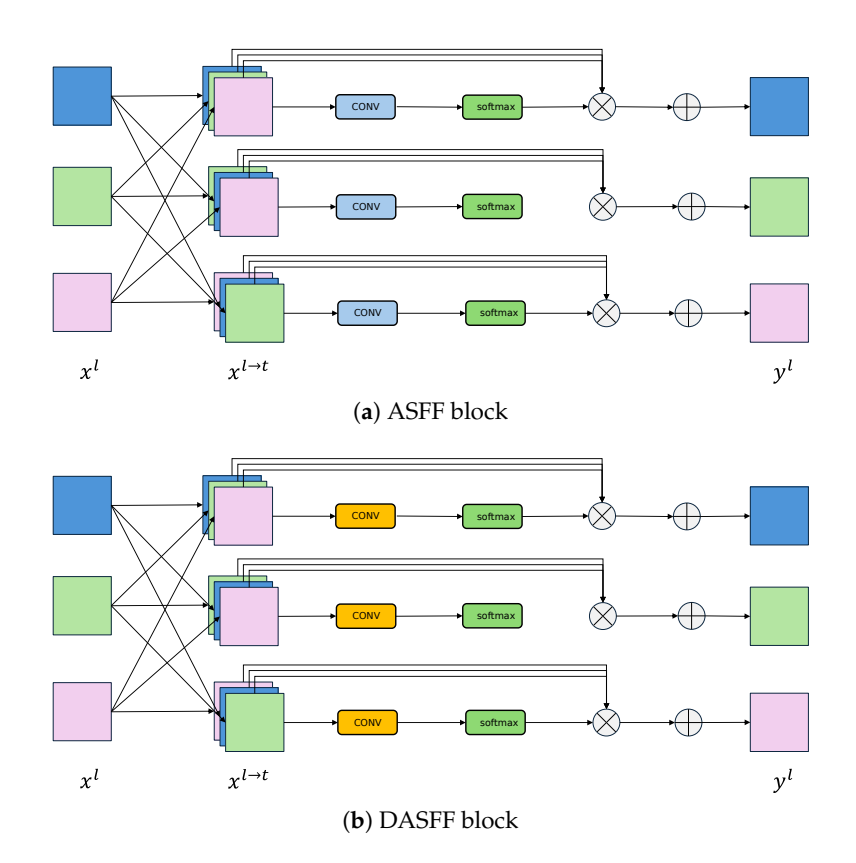


Figure 9. Comparison between ASFF and DASFF.

2.5. Loss Function

The CIoU loss function commonly used in YOLO series algorithms has certain limitations when addressing challenges such as small objects, complex backgrounds, and class imbalance. Insulator defect detection is a typical small-object detection task often set in cluttered environments. Moreover, variations in lighting conditions, aerial shooting distances, and camera angles can lead to significant differences in image quality, resulting in an imbalance between low-quality and high-quality samples. These factors further degrade the accuracy and robustness of insulator defect detection in real-world applications.

To improve the network's convergence speed and detection accuracy, this paper proposes a combined loss function that integrates Wise-IoUv3 and Focal Loss [31]. Wise-IoUv3 uses a dynamic non-monotonic focusing mechanism to adaptively weight anchor boxes based on quality, reducing low-quality interference and improving localization. Focal Loss mitigates class imbalance by focusing on hard samples. Together, they jointly optimize regression and classification, enhancing overall performance and training stability.

Wise-IoUv3 is an improved bounding box regression loss function that introduces a dynamic non-monotonic focusing mechanism to intelligently assess anchor quality and dynamically adjust gradient allocation. This reduces the negative impact of low-quality anchors during training, enhances the model's focus on medium-quality anchors, and improves overall detection performance. The expression for the non-monotonic focusing Wise–IoUv3 loss function is as follows:

$$L_{WIoUv3} = \frac{\lambda}{\kappa \mu^{\lambda - \kappa}} \times \exp\left[\frac{(u - u_{gt})^2 + (v - v_{gt})^2}{(S_w^2 + S_h^2)^*}\right] \times L_{IoU}$$
(3)

where $\lambda = \frac{L_{loU}^*}{L_{loU}}$ is the outlier adjustment factor, which represents the quality of the anchor box, while $\lambda \in [0, +\infty)$. κ, μ are model learning parameters, (u, v) are the predicted box center coordinates, and (u_{gt}, v_{gt}) are the ground truth box center coordinates. S_w , S_h

represents the size of the minimum bounding box; the superscript * indicates that S_w and S_h are detached from the computation graph. L_{IoU} is the generalized IoU loss, used to evaluate and optimize the matching degree between predicted bounding boxes and ground truth bounding boxes. Focal Loss helps handle class imbalance by focusing training on hard-to-classify examples and reducing the impact of easy ones, improving model performance on difficult samples. The expression for the Focal Loss function is as follows:

$$L_{Focal} = -\alpha_t (1 - p_t)^{\beta_t} \log(p_t) \tag{4}$$

where α_t is the class balancing factor, β_t stands for the focusing factor, and p_t is the predicted probability of the model for a certain class.

The combination of Wise–IoUv3 and Focal can enhance the model's convergence speed, focus on small targets, and select low-quality samples, thereby improving the model's generalization performance. The loss function designed in this paper is as follows:

$$L_{\text{loss}} = \frac{1}{1 + \exp(-kt + b)} L_{WIoUv3} + \left(1 - \frac{1}{1 + \exp(-kt + b)}\right) L_{Focal}$$
 (5)

where k,b are hyper-parameters controlling weight dynamics, t denotes the number of epochs during training, and $\frac{1}{1+\exp(-kt+b)}$ is the adaptive weight for the regression-classification balance.

3. Results and Analysis

3.1. Experimental Preparation

Experimental Environment: The experiment was conducted locally, and the experimental environment is shown in Table 1.

Table 1. Experimental environment.

CPU	GPU	System	Python Version	Pytorch Version	CUDA Version
i5 13600kf	NVIDIA GeForce RTX3090	Ubuntu 24.04	3.12	2.6	12.8

Experimental Data: To improve the model's generalization ability, the transmission line insulator defect dataset used in this paper consists of two parts, with a total of 4648 images. The dataset is randomly split into training, validation, and testing sets in a 7:2:1 ratio. The first part is a self-built dataset containing 3800 insulator images sized 640 × 640 pixels. As shown in Figure 10, these images were captured across different regions using drones and cameras, then stitched to form composites with multiple insulators. This enhances data diversity and complexity. The dataset includes various environmental conditions and viewpoints, reflecting real-world challenges such as lighting changes, occlusions, and complex backgrounds. The second part is the CPLID public dataset [5], which contains 848 images of insulators. These images include complete insulator string images from real-world scenarios. The dataset used in this paper not only contains subtle defect features of the insulators but also includes complex backgrounds found in real-world environments, thus the experimental results can better reflect the quality of insulator defect detection in real environments.











Figure 10. Images of the dataset.

The model's training hyperparameters are shown in Table 2.

Table 2. Hyperparameter setting.

Input Image Size	Learning Rate	Momentum	Optimizer	Weight Decay Coefficient	Number of Iterations
640 × 640	0.001	0.937	AdamW	0.0005	600

3.2. Evaluation Metrics

In this paper, the model's detection performance is evaluated using metrics such as precision (P), recall (R), and Mean Average Precision (mAP), and the mathematical expressions are as follows:

$$P = \frac{TP}{TP + FP} \tag{6}$$

$$R = \frac{TP}{TP + FN} \tag{7}$$

$$mAP = \frac{1}{n} \sum_{i=1}^{n} AP_i \tag{8}$$

$$AP = \int_{0}^{1} P(R)dR \tag{9}$$

where *TP* represents the number of true positives correctly identified as positive, *FP* represents the number of false positives incorrectly identified as positive, and *FN* denotes the number of false negatives incorrectly identified as negative. *AP* is the Average Precision for a single class, calculated as the area under the precision–recall (*TP*) curve. *mAP* is the mean value across all classes, with higher values indicating better model precision.

3.3. Ablation Experiment

To verify the advantages of the proposed DGNCA-Net model in insulator defect detection, an ablation experiment is conducted based on the YOLOv11 model. The experimental results are shown in Table 3.

Table 3. Results of ablation study.

Ghost- Backbone	DC-PUFPN	L_{loss}	P%	R%	mAP50%
Dackbone					
-	-	-	86.52	74.89	81.67
\checkmark	-	-	88.37	76.12	82.25
-	\checkmark	-	88.14	76.41	82.57
-	-	\checkmark	87.21	76.53	82.04
\checkmark	\checkmark	-	89.92	77.85	83.95
\checkmark	-	\checkmark	90.74	78.41	84.32
-	\checkmark	\checkmark	90.18	78.16	84.17
\checkmark	\checkmark	\checkmark	91.07	79.21	85.46

The model was trained using the same training data and hyperparameter settings. After 600 epochs, the evaluation metrics P, R, and mAP were calculated on the same test set. Based on the results from the eight experimental groups mentioned above, it can be clearly observed that the progressive integration of the Ghost-Backbone, DC-PUFPN, and $L_{\rm loss}$ components significantly improves model performance. Starting from the baseline, the individual addition of Ghost-Backbone, DC-PUFPN, and $L_{\rm loss}$ led to steady increases in P, R, and mAP. When combining any two of these modules, the performance continued to improve, demonstrating their complementary effects. Finally, the complete integration of all three modules resulted in the highest performance, with P, R, and mAP reaching 91.07%, 79.21%, and 85.46%, respectively. Compared to the baseline, this reflects improvements of 4.55%, 4.32%, and 3.79%. These results confirm that the proposed DGNCA-Net achieves a substantial cumulative gain in detection accuracy through the joint contribution of each component.

3.4. Comparative Experiments

YOLOv7-tiny [35]

To comprehensively evaluate the superiority of the proposed DGNCA-Net model in terms of model size, computational complexity, and insulator defect detection accuracy, a comparison was made with four different defect detection models under the same dataset and hardware environment. The compared deep learning models and the comparison results are shown in Table 4 and Figure 11.

Model	P%	R%	mAP50%	Parameters (M)	GFLOPs
DGNCA-Net	91.07	79.21	85.46	2.88	3.97
YOLO-PowerLite [32]	78.35	70.12	74.21	1.73	5.60
YOLO-HF [33]	80.20	70.61	74.36	6.59	31.5
YOLOv8n [34]	86.12	75.16	82.60	3.15	4.43
YOLOv7 [35]	84.51	74.52	80.91	36.9	104.7

76.29

78.84

6.20

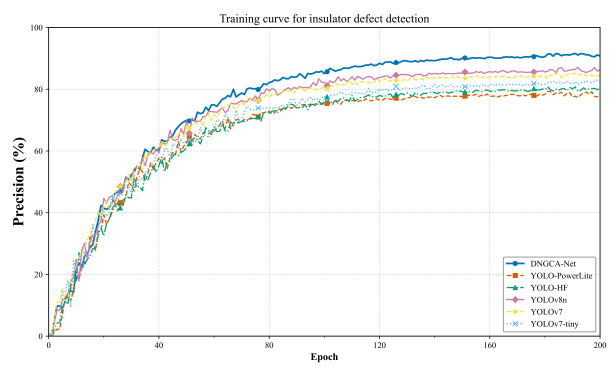
3.50

Table 4. Comparative experimental results of different models.

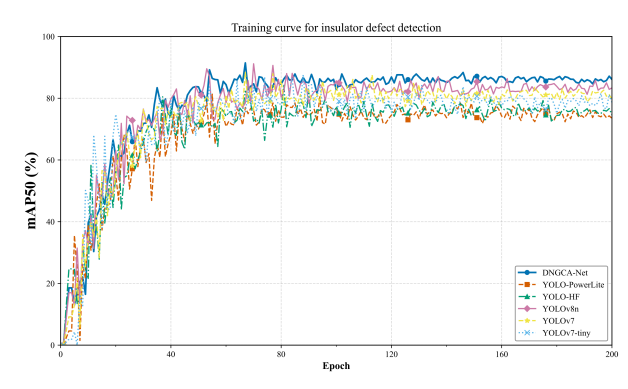
82.13

In addition to evaluating the model's accuracy in insulator defect detection using P, R, and mAP, we introduce two additional metrics: the number of parameters and GFLOPs, to comprehensively assess the model's scale and computational complexity. The number of parameters represents the total count of trainable weights in the model—higher values indicate a more complex structure. A lower GFLOPs value signifies reduced computational complexity and lighter computational load.

Based on the comparative results of *P*, *R*, and *mAP*, the proposed DGNCA-Net algorithm outperforms models such as YOLO-PowerLite, YOLO-HF, YOLOv8n, YOLOv7, and YOLOv7-tiny in defect detection accuracy, while maintaining a smaller parameter size. This reflects a well-balanced design between lightweight architecture and detection performance. In achieving higher accuracy, DGNCA-Net also significantly reduces the number of parameters and computational overhead, making it more suitable for deployment on resource-constrained edge devices or in real-time scenarios. Therefore, DGNCA-Net not only ensures reliable detection performance but also demonstrates excellent efficiency and adaptability, offering a more practical and effective solution for real-world engineering applications.



(a) The variation curve of Accuracy



(b) The variation curve of *mAP*50%

Figure 11. Model performance comparison.

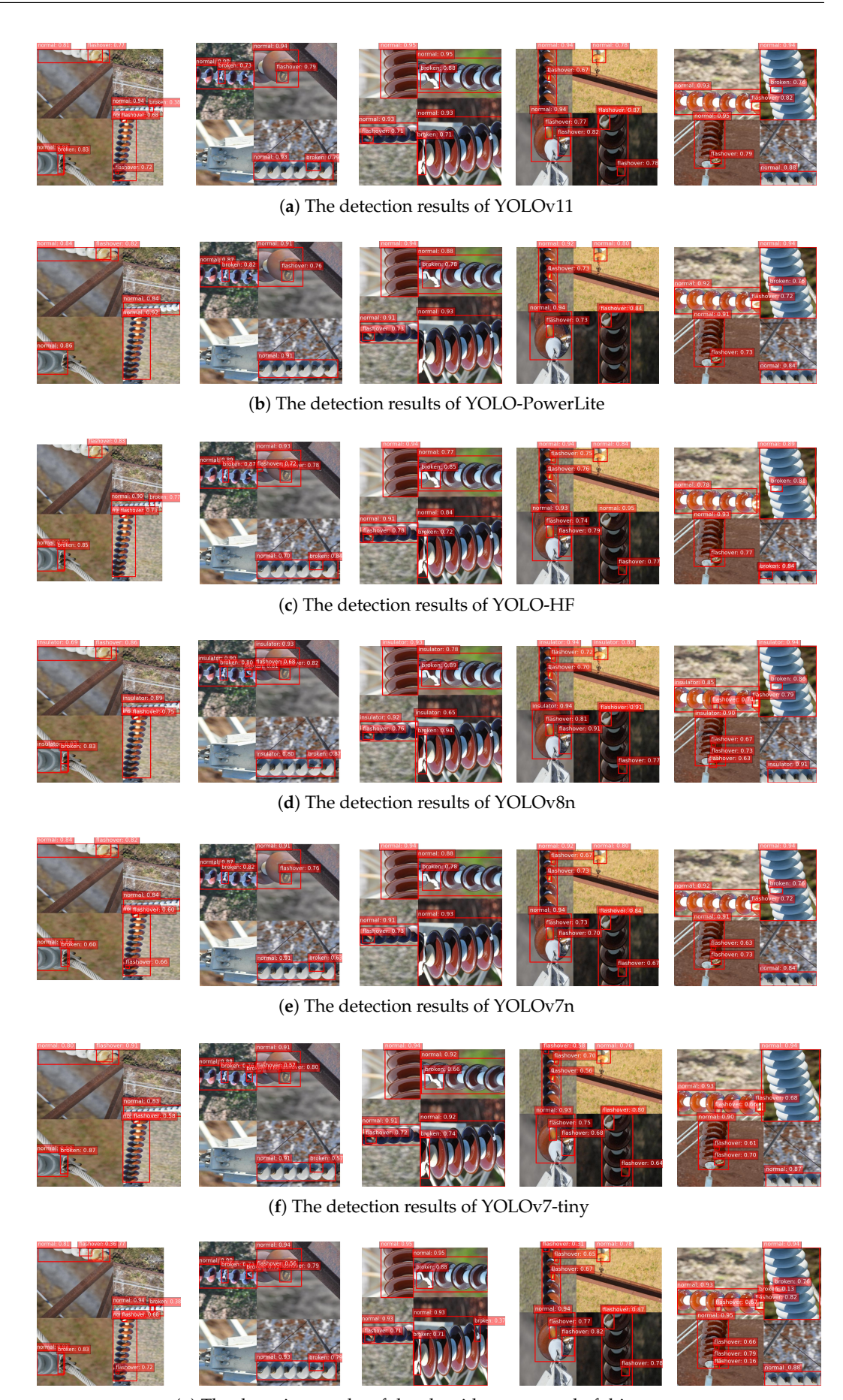
3.5. Visualization Comparison Experiment

To further verify the superiority of the proposed algorithm, the visual comparison results of insulator defect detection between the algorithm proposed in this study, the YOLOv11 algorithm, and the algorithms listed in Table 4 are presented in Figure 12.

Based on the results presented in Figure 12 and Table 5, the proposed DGNCA-Net demonstrates superior detection performance compared to other mainstream models. It is the only model that achieves zero missed detections across all categories. In contrast, other models such as YOLOv11 and YOLO-PowerLite exhibit significantly higher total missed cases, with 12 and 19, respectively. Even lightweight detectors like YOLOv8-n and YOLOv7-tiny show total misses of 8 and 9. These results highlight the robustness and reliability of DGNCA-Net, especially in accurately identifying challenging defect types. Overall, the findings confirm that DGNCA-Net offers substantial improvements in detection completeness and is highly suitable for real-world insulator defect detection scenarios where precision is critical.

Table 5. Missing cases by category and total number per model.

Model	Normal	Flashover	Broken	Total Miss
Ground Truth	19	19	10	-
YOLOv11	19	10	7	12
YOLO-PowerLite	19	7	3	19
YOLO-HF	19	10	8	11
YOLOv8-n	19	15	6	8
YOLOv7-n	19	13	5	11
YOLOv7-tiny	19	14	6	9
DGNCA-Net	19	19	10	0



 (\boldsymbol{g}) The detection results of the algorithm proposed of this paper

Figure 12. Visualization results comparison.

4. Conclusions

This paper proposes a lightweight insulator defect detection algorithm, DGNCA-Net, based on the YOLOv11 framework. By integrating an improved Ghost-based backbone, the DC-PUFPN neck network, and a refined loss function, the model effectively enhances both detection accuracy and computational efficiency for multi-scale small target defects in insulators. The research offers a lightweight and high-precision solution for power line inspections, significantly reducing manual inspection costs and safety risks, and holds important practical value for improving the intelligence level of power grid operation and maintenance. Although the proposed method demonstrates excellent detection performance, there are still some challenges to be addressed in real-world applications: (1) under extreme weather conditions (e.g., strong backlighting, rain, or snow), image quality significantly degrades, which affects the model's detection accuracy and stability. (2) In cluttered backgrounds or scenarios where insulators are densely arranged, target overlap and occlusion may occur, hindering accurate localization and identification of defects. Future work will focus on enhancing the model's adaptability to complex environments and improving its robustness against image noise and interference in extreme scenarios, in order to further increase its practicality.

Author Contributions: Conceptualization, Q.C. and Y.M.; methodology, Q.C., Y.L. and Y.M.; software, Y.M.; validation, W.Y. and R.Z.; formal analysis, Y.L.; investigation, Q.C. and Y.M.; resources, Y.L.; data curation, Y.L.; writing—original draft preparation, Q.C.; writing—review and editing, Y.M.; visualization, Y.M.; supervision, R.Z.; project administration, Q.C. and Y.M.; funding acquisition, Q.C. All authors have read and agreed to the published version of this manuscript.

Funding: This research was funded by Technology projects of China Southern Power Grid Co., Ltd. (grant number CGYKJXM20230142).

Institutional Review Board Statement: Not applicable.

Informed Consent Statement: Not applicable.

Data Availability Statement: The datasets presented in this article are not readily available because they contain proprietary information protected under contractual agreements with the collaborating company. Requests to access the datasets should be directed to the corresponding author.

Acknowledgments: We wish to thank all of participants who supported our study and the reviewers for their constructive suggestions on this manuscript.

Conflicts of Interest: Author Qiang Chen, Yuanfeng Luo, Wu Yuan, Ruiliang Zhang were employed by the China Southern Power Grid Company. The remaining authors declare that the research was conducted in the absence of any commercial or financial relationships that could be construed as a potential conflict of interest.

Abbreviations

The following abbreviations are used in this manuscript:

CSG China Southern power Grid

EHV Extra-High Voltage

References

- 1. Wang, Q.; Hu, Z.; Li, E.; Wu, G.; Yang, W.; Hu, Y.; Peng, W.; Sun, J. YOLOLS: A Lightweight and High-Precision Power Insulator Defect Detection Network for Real-Time Edge Deployment. *Energies* **2025**, *18*, 1668. [CrossRef]
- 2. Ji, Y.; Zhang, D.; He, Y.; Zhao, J.; Duan, X.; Zhang, T. Improved YOLO11 Algorithm for Insulator Defect Detection in Power Distribution Lines. *Electronics* **2025**, *14*, 1201. [CrossRef]
- 3. Zhao, J.; Miao, S.; Kang, R.; Cao, L.; Zhang, L.; Ren, Y. Insulator Defect Detection Algorithm Based on Improved YOLOv11n. Sensors 2025, 25, 1327. [CrossRef]

4. She, L.; Fan, Y.; Xu, M.; Wang, J.; Xue, J.; Ou, J. Insulator Breakage Detection Utilizing a Convolutional Neural Network Ensemble Implemented With Small Sample Data Augmentation and Transfer Learning. *IEEE Trans. Power Deliv.* **2022**, *37*, 2787–2796. [CrossRef]

- 5. Tao, X.; Zhang, D.; Wang, Z.; Liu, X.; Zhang, H.; Xu, D. Detection of Power Line Insulator Defects Using Aerial Images Analyzed With Convolutional Neural Networks. *IEEE Trans. Syst. Man Cybern. Syst.* **2020**, *50*, 1486–1498. [CrossRef]
- 6. Lin, Y.; Tian, L.; Du, Q. Automatic Overheating Defect Diagnosis Based on Rotated Detector for Insulator in Infrared Image. *IEEE Sens. J.* **2023**, 23, 26245–26258. [CrossRef]
- 7. Han, Y.; Liu, Z.; Lee, D.; Liu, W.; Chen, J.; Han, Z. Computer vision–based automatic rod-insulator defect detection in high-speed railway catenary system. *Int. J. Adv. Robot. Syst.* **2018**, *15*, 1729881418773943. [CrossRef]
- 8. Zhang, D.; Gao, S.; Yu, L.; Kang, G.; Wei, X.; Zhan, D. DefGAN: Defect Detection GANs With Latent Space Pitting for High-Speed Railway Insulator. *IEEE Trans. Instrum. Meas.* **2021**, *70*, 1–10. [CrossRef]
- 9. Liu, S.; Ma, Y.; Zheng, Z.; Xinfu, P.; Li, B. Insulator Defect Recognition Based on Vision Big-Model Transfer Learning and Stochastic Configuration Network. *IET Signal Process.* **2024**, 2024, 4182652. [CrossRef]
- 10. Xu, S.; Che, C. Detection of defects in composite insulators based on laser induced plasma combined with machine learning. *Microw. Opt. Technol. Lett.* **2024**, *66*, e34298. [CrossRef]
- 11. Li, D.; Lu, Y.; Gao, Q.; Li, X.; Yu, X.; Song, Y. LiteYOLO-ID: A Lightweight Object Detection Network for Insulator Defect Detection. *IEEE Trans. Instrum. Meas.* **2024**, *73*, 1–12. [CrossRef]
- 12. Chen, Y.; Deng, C.; Sun, Q.; Wu, Z.; Zou, L.; Zhang, G.; Li, W. Lightweight Detection Methods for Insulator Self-Explosion Defects. Sensors 2024, 24, 290. [CrossRef] [PubMed]
- 13. Qiu, Z.; Zhu, X.; Liao, C.; Shi, D.; Qu, W. Detection of Transmission Line Insulator Defects Based on an Improved Lightweight YOLOv4 Model. *Appl. Sci.* **2022**, *12*, 1207. [CrossRef]
- 14. Cao, Z.; Chen, K.; Chen, J.; Chen, Z.; Zhang, M. CACS-YOLO: A Lightweight Model for Insulator Defect Detection Based on Improved YOLOv8m. *IEEE Trans. Instrum. Meas.* **2024**, *73*, 1–10. [CrossRef]
- 15. Lu, Y.; Li, D.; Li, D.; Li, X.; Gao, Q.; Yu, X. A Lightweight Insulator Defect Detection Model Based on Drone Images. *Drones* **2024**, 8, 431. [CrossRef]
- 16. Jiang, Y.; Wang, S.; Cao, W.; Liang, W.; Shi, J.; Zhou, L. RDB-YOLOv8n: Insulator defect detection based on improved lightweight YOLOv8n model. *J. Real-Time Image Process.* **2024**, *21*, 178. [CrossRef]
- 17. Liu, C.; Yi, W.; Liu, M.; Wang, Y.; Hu, S.; Wu, M. A Lightweight Network Based on Improved YOLOv5s for Insulator Defect Detection. *Electronics* **2023**, *12*, 4292. [CrossRef]
- 18. Han, W.; Cai, Z.; Li, X.; Ding, A.; Zou, Y.; Wang, T. LMD-YOLO: A lightweight algorithm for multi-defect detection of power distribution network insulators based on an improved YOLOv8. *PLoS ONE* **2025**, *20*, e0314225. [CrossRef]
- 19. Wei, L.; Jin, J.; Deng, K.; Liu, H. Insulator defect detection in transmission line based on an improved lightweight YOLOv5s algorithm. *Electr. Power Syst. Res.* **2024**, 233, 110464. [CrossRef]
- 20. He, Z.; Wang, Y.; Zheng, A.; Liu, J.; Lou, T.; Zhang, J.; Jiang, P.; Xu, J. Insulator defect detection algorithm based on adaptive feature fusion and lightweight YOLOv5s. *J. Real-Time Image Process.* **2025**, 22, 12. [CrossRef]
- 21. Zhang, Q.; Zhang, J.; Li, Y.; Zhu, C.; Wang, G. ID-YOLO: A Multimodule Optimized Algorithm for Insulator Defect Detection in Power Transmission Lines. *IEEE Trans. Instrum. Meas.* **2025**, *74*, 1–11. [CrossRef]
- 22. Gong, C.; Jiang, W.; Zou, D.; Weng, W.; Li, H. An Insulator Fault Diagnosis Method Based on Multi-Mechanism Optimization YOLOv8. *Appl. Sci.* **2024**, *14*, 8770. [CrossRef]
- 23. Liu, B.; Jiang, W. LA-YOLO: Bidirectional Adaptive Feature Fusion Approach for Small Object Detection of Insulator Self-Explosion Defects. *IEEE Trans. Power Deliv.* **2024**, *39*, 3387–3397. [CrossRef]
- 24. Li, Z.; Jiang, C.; Li, Z. An Insulator Location and Defect Detection Method Based on Improved YOLOv8. *IEEE Access* **2024**, 12, 106781–106792. [CrossRef]
- 25. Xu, Z.Y.; Tang, X. Transmission line insulator defect detection algorithm based on MAP-YOLOv8. *Sci. Rep.* **2025**, *15*, 10288. [CrossRef]
- 26. Kisantal, M.; Wojna, Z.; Murawski, J.; Naruniec, J.; Cho, K. Augmentation for small object detection. *arXiv* **2019**, arXiv:1902.07296. [CrossRef]
- 27. Wang, Z.; Su, Y.; Kang, F.; Wang, L.; Lin, Y.; Wu, Q.; Li, H.; Cai, Z. PC-YOLO11s: A Lightweight and Effective Feature Extraction Method for Small Target Image Detection. *Sensors* **2025**, 25, 348. [CrossRef] [PubMed]
- 28. Khanam, R.; Hussain, M. YOLOv11: An Overview of the Key Architectural Enhancements. *arXiv* **2024**, arXiv:2410.17725. [CrossRef]
- 29. Ding, X.; Zhang, X.; Han, J.; Ding, G. Scaling Up Your Kernels to 31 × 31: Revisiting Large Kernel Design in CNNs. In Proceedings of the 2022 IEEE/CVF Conference on Computer Vision and Pattern Recognition (CVPR), New Orleans, LA, USA, 18–24 June 2022; pp. 11953–11965. [CrossRef]

30. Han, K.; Wang, Y.; Tian, Q.; Guo, J.; Xu, C.; Xu, C. GhostNet: More Features From Cheap Operations. In Proceedings of the 2020 IEEE/CVF Conference on Computer Vision and Pattern Recognition (CVPR), Seattle, WA, USA, 13–19 June 2020; pp. 1577–1586. [CrossRef]

- 31. Tong, Z.; Chen, Y.; Xu, Z.; Yu, R. Wise-IoU: Bounding Box Regression Loss with Dynamic Focusing Mechanism. *arXiv* 2023, arXiv:cs.CV/2301.10051.
- 32. Liu, C.; Wei, S.; Zhong, S.; Yu, F. YOLO-PowerLite: A Lightweight YOLO Model for Transmission Line Abnormal Target Detection. *IEEE Access* **2024**, *12*, 105004–105015. [CrossRef]
- 33. Peng, B.; Kim, T.K. YOLO-HF: Early Detection of Home Fires Using YOLO. IEEE Access 2025, 13, 79451–79466. [CrossRef]
- 34. Varghese, R.; Sambath, M. YOLOv8: A Novel Object Detection Algorithm with Enhanced Performance and Robustness. In Proceedings of the 2024 International Conference on Advances in Data Engineering and Intelligent Computing Systems (ADICS), Chennai, India, 18–19 April 2024; pp. 1–6. [CrossRef]
- 35. Wang, C.Y.; Bochkovskiy, A.; Liao, H.Y.M. YOLOv7: Trainable Bag-of-Freebies Sets New State-of-the-Art for Real-Time Object Detectors. In Proceedings of the 2023 IEEE/CVF Conference on Computer Vision and Pattern Recognition (CVPR), Vancouver, BC, Canada, 17–24 June 2023; pp. 7464–7475. [CrossRef]

Disclaimer/Publisher's Note: The statements, opinions and data contained in all publications are solely those of the individual author(s) and contributor(s) and not of MDPI and/or the editor(s). MDPI and/or the editor(s) disclaim responsibility for any injury to people or property resulting from any ideas, methods, instructions or products referred to in the content.